Role for Lysine 142 in the Excision of Adenine from A:G Mispairs by MutY DNA Glycosylase of *Escherichia coli*†

Dmitry O. Zharkov,[‡,§] Rotem Gilboa,[||] Ishay Yagil,[||] Jadwiga H. Kycia,[⊥] Sue Ellen Gerchman,[⊥] Gil Shoham,[||] and Arthur P. Grollman*[,‡]

Laboratory of Chemical Biology, Department of Pharmacological Sciences, State University of New York at Stony Brook, Stony Brook, New York 11794, USA, Novosibirsk Institute of Bioorganic Chemistry, Siberian Division of Russian Academy of Sciences, Prospect Lavrentieva 8, Novosibirk 630090, Russia, Department of Inorganic Chemistry and Laboratory for Structural Chemistry and Biology, Hebrew University of Jerusalem, Jerusalem 91904, Israel, and Biology Department, Brookhaven National Laboratory, Upton, New York 11973, USA

Received July 5, 2000; Revised Manuscript Received September 27, 2000

ABSTRACT: MutY participates in the repair of oxidatively damaged DNA by excising adenine from dA:dG and dA:8-oxodG mispairs; this DNA glycosylase can be cross-linked to DNA through Lys-142. We have investigated the properties of a mutant protein in which Lys-142 is replaced by glutamine. Using the rifampicin resistance assay, MutY K142Q was shown to complement the *mutY* mutator phenotype to the same extent as wild-type MutY. Although MutY K142Q does not form a Schiff base with DNA, it retains in part the catalytic properties of wild-type enzyme. The K142Q mutation selectively impairs processing of DNA containing dA:dG mispairs but not that of substrates containing dA:8-oxodG. Decreased substrate processing is mediated primarily via an increase in K_D (21.8 nM for MutY vs 298 nM for MutY K142Q). The catalytic constant, measured in single turnover experiments, was not significantly affected. At pH < 6.0, the activity of MutY K142Q on the dA:dG mispair was approximately the same as for wild-type protein, suggesting that a dG(anti) to dG(syn) transition is effected at low pH. The three-dimensional structure of the catalytic domain of MutY K142Q, determined at 1.35 Å resolution, shows no significant differences between wild-type and mutant protein, indicating that Lys-142 is not critical for maintaining the conformation of MutY. We conclude that Lys-142 recognizes guanine in the dA:dG mispair, helping position this residue in the syn conformation and facilitating binding of substrate DNA. Lys-142 is not involved in the catalytic steps of base excision.

A variety of mutagenic and cytotoxic lesions in DNA are generated by reactive oxygen species, one of the most abundant of these being 8-oxoguanine (*1*, *2*). During DNA replication, 8-oxodG[1] pairs with dC and dA (*3*). The 8-oxodG:dA mispair leads to G:C → T:A transversions when 8-oxodG is in the template strand and to A:T → C:G transversions when the modified base is introduced via 8-oxodGTP, itself generated by reactive oxygen species (*4*, *5*).

In *Escherichia coli*, three DNA repair enzymes work in concert to minimize the mutagenic consequences of 8-oxodG (*6*, *7*). MutT is an 8-oxodGTPase that cleanses the cellular deoxynucleoside triphosphate pool (*8*). Fpg (MutM) is a DNA glycosylase/AP lyase that acts preferentially on 8-oxodG:dC, excising 8-oxoG from oxidatively damaged DNA (*9*). MutY is an adenine DNA glycosylase that acts preferentially on 8-oxodG:dA in a DNA replication intermediate, initiating a process by which the oxidized base subsequently can be excised by Fpg (*10*, *11*). Initially, MutY was characterized as a DNA glycosylase that removes adenine from dA:dG mispairs (*12*, *13*); later, it was shown to act preferentially on dA:8-oxodG mispairs (*10*, *11*, *14*, *15*). A primary function of MutY appears to be to minimize 8-oxoG-mediated mutagenesis in cells (*16*). Sequence analysis (*17*) and establishment of the three-dimensional structure (*18*) place MutY in the endonuclease III (Endo III) family of DNA repair glycosylases (*19*).

DNA glycosylases/AP lyases that excise the damaged base and nick DNA by β-elimination form covalent intermediates that can be trapped by reduction with $NaBH_4$ (*20*). The covalent intermediate, a Schiff base involving a free amino group in the enzyme's active site and C1′ of deoxyribose in the target nucleoside, is a prerequisite for β-elimination. Previous studies of the reaction mechanism revealed that MutY is capable of forming a Schiff base (*21*−*23*) but has little, if any AP lyase activity (*23*, *24*; for reviews and apparent resolution of this controversial issue, see refs *23* and *25*).

† Research supported by a grant (CA-17395) from the National Institutes of Health.

* To whom correspondence should be addressed. E-mail: apg@pharm.sunysb.edu, fax: (631) 444-7641.

‡ State University of New York at Stony Brook.

§ Novosibirsk Institute of Bioorganic Chemistry.

|| Hebrew University of Jerusalem.

⊥ Brookhaven National Laboratory.

[1] Abbreviations: AP, apurinic/apyrimidinic; carba-dA, 2′-deoxyaristeromycin; Endo III, endonuclease III; F, 3-hydroxy-2-hydroxymethyltetrahydrofuran; 8-oxo-carba-dG, 8-oxo-7,8-dihydro-2′-deoxy-1′,4′-carbaguanosine; 8-oxodG, 8-oxo-7,8-dihydro-2′-deoxyguanosine; 8-oxoG, 8-oxo-7,8-dihydroguanine; PAGE, polyacrylamide gel electrophoresis

10.1021/bi001538k CCC: $19.00
Published on Web 10/27/2000

AP lyases of the Endo III family possess a conserved lysine residue that forms the Schiff base and is absolutely necessary for β-elimination; in MutY, Ser-120 is found in this position and cross-linking is mediated by the nearby Lys-142 (*23*). Schiff base formation was recently reported to be disposable for enzymatic activity, since MutY K142A mutants process dA:8-oxodG mispair as efficiently as the wild-type protein (*26*). To clarify the role of Lys-142 in the reaction mechanism of MutY, we have replaced this residue with alanine, glutamine, or arginine and compared the mutant proteins with wild-type MutY with respect to their catalytic properties. The glutamine mutant (MutY K142Q) was investigated with respect to its kinetics, ability to suppress mutations, and three-dimensional structure. Results of these studies indicate that Lys-142 is not directly involved in catalyzing base excision and is not essential for maintaining the structure or conformation of MutY but is critically important in recognizing guanine in a dA:dG mispair.

EXPERIMENTAL PROCEDURES

Oligodeoxynucleotides and Enzymes. Phosphoramidites of 8-oxodG, carba-dA, 8-oxo-carba-dG and an abasic site analogue 3-hydroxy-2-hydroxymethyl-tetrahydrofuran (F) were synthesized according to published procedures (*27*−*29*); other deoxynucleotide phosphoramidites were purchased from Glen Research. Oligodeoxynucleotides were synthesized on an Applied Biosystems model 394 automated DNA synthesizer and purified by denaturing PAGE and reverse phase HPLC. Oligodeoxynucleotides used as substrates or ligands for MutY were 23-mers with the sequence d(CTCTCCTTCXCTCCTTTCCTCT), where X = dA, carba-dA, F, dU, or 8-oxo-carba-dG, labeled at the 5′-end using [γ-^{32}P]-ATP (Amersham) and T4 polynucleotide kinase and annealed to the corresponding complementary strand in a 1:1.3 ratio. The complementary strand contained dG, 8-oxodG, T, or dC opposite X. To obtain duplex DNA containing a natural AP site opposite dG or 8-oxodG, the corresponding duplex containing dU was treated with 0.01 U/μL of uracil-DNA glycosylase for 30 min at 37 °C in the standard reaction buffer (see below); this substrate was used immediately. T4 polynucleotide kinase, Klenow fragment, T4 DNA ligase, restriction endonucleases, and uracil-DNA glycosylase were purchased from New England Biolabs, Pfu DNA polymerase and PCR reagents from Stratagene, and lysozyme from Sigma-Aldrich.

Overexpression and Purification of MutY. Full-length MutY was amplified from *E. coli* BL21 genomic DNA by PCR using *Pfu* DNA polymerase. The upstream primer contained a *Nde*I restriction site and an ATG start codon, and the downstream primer contained a translation stop codon and a *Bam*HI restriction site. The amplified gene was subcloned into the *Nde*I−*Bam*HI site of the expression vector pET13a (*30*). The sequence was verified using standard fluorescent DNA sequencing techniques. A p25 domain of MutY (Met-1−Lys-225) was amplified from the full-length clone and inserted into pET13a. The upstream primer used for PCR was the same as for the full-length clone, and the downstream primer contained a translation stop codon and *Bam*HI restriction site but ended at Lys-225. The K142A, K142Q, and K142R mutants of MutY and MutY p25 were made using the QuikChange site-directed mutagenesis kit (Stratagene). The initial mutagenesis was done using truncated MutY as template. After sequence verification, the MutY *Nde*I−*Sac*II fragment containing the mutation was moved into a wild-type background of both the full-length and the truncated clone and sequenced again. Both full-length and truncated MutY containing the mutation of interest were obtained using *E. coli* overexpression strain B834(DE3) (Novagen).

To purify full-length MutY, YT×2 medium (1 L) containing 25 μg/mL kanamycin was inoculated with 20 mL of an overnight culture of *E. coli* B834(DE3) harboring an appropriate pET13a MutY plasmid. The culture was grown at 37 °C with shaking for 2 h, and then allowed to equilibrate at 30 °C with shaking for 1 h. IPTG was added to a final concentration of 50 μM, and cells were incubated for 5 h at 30 °C with shaking, harvested by centrifugation at 12000*g* at 4 °C, and stored frozen at −80 °C. After thawing the sample, the pellet (3−4 g of wet weight) was resuspended in TE buffer, pH 8.0 (20 mL final volume), supplemented with 1 mM phenylmethylsulfonyl fluoride. Lysozyme was added to a final concentration of 50 μg/mL, followed by stirring for 20 min at room temperature. NaCl (final concentration 1 M) and DNase I (final concentration 0.5 μg/mL) were then added, and the suspension was stirred for another 20 min. Cell debris was removed by centrifugation at 17000*g* at 4 °C. The supernatant was treated with 200 μL of 5% polyethylenimine solution, and the centrifugation step was repeated. The supernatant was then diluted with 4 vol of buffer A (50 mM HEPES-NaOH, pH 8.0, 1 mM Na-EDTA, and 1 mM DTT), centrifuged for 30 min at 12000*g* at 4 °C, and loaded onto a Fractogel EMD SO_3^- 650 column (15 mL) equilibrated with buffer A containing 200 mM NaCl. The protein was eluted using a 180-mL gradient of 200−800 mM NaCl in buffer A. The main A_{280} absorption peak (eluted at about 470 mM NaCl) was collected and loaded directly on a Superdex 75 HR 10/30 column (Pharmacia) equilibrated with buffer A containing 400 mM NaCl. Fractions were analyzed by SDS−PAGE with Coomassie Blue staining. Fractions with at least 95% pure protein were pooled, dialyzed against the storage buffer (10 mM Tris-HCl, pH 7.5, 400 mM NaCl, 50% glycerol), and stored at −20 °C. Protein concentrations were determined by Bradford assay, using BSA as a standard.

To purify the MutY p25 fragment, TBY medium (1 L) containing 25 μg/mL kanamycin was inoculated with 20 mL of an overnight culture of *E. coli* B834(DE3) harboring an appropriate pET13a MutY plasmid. The culture was grown at 37 °C with shaking until A_{600} = 0.8−0.9, and IPTG was added to a final concentration of 400 μM. Cells were harvested after 3 h by centrifugation and stored at −80 °C. To produce selenomethionyl-containing protein derivatives, the cultures were grown in minimal medium M9×2 containing 0.4% glucose and supplemented with amino acids except methionine and L-selenomethionine at 40 mg/L and vitamins at 1 mg/L (*31*). After thawing, cells (5 g) were resuspended in 40 mL of the buffer containing 20 mM sodium phosphate, pH 7.8, and 1 M NaCl, and disrupted by sonication. The lysate treatment and chromatographic steps were performed as described above except EDTA and DTT were omitted, and 20 mM sodium phosphate, pH 7.8, was used instead of HEPES buffer during cation exchange chromatography. The fractions containing MutY were combined, concentrated to

2 mg/mL using a Centricon-10 device (Amicon), and used immediately in crystallization experiments.

Cross-linking of Oligonucleotide Substrate to MutY. Reaction mixtures (10 μL) containing 20 nM ^{32}P-labeled 23-mer duplex DNA with a dA:8-oxodG pair and 30 ng of MutY were incubated for 30 min at 37 °C in a buffer containing 25 mM sodium phosphate, pH 6.8, and 50 mM freshly dissolved $NaBH_4$. SDS loading buffer (10 μL) was added, and reactions were terminated by heating for 5 min at 95 °C. Aliquots (18 μL) were loaded onto 12% discontinuous SDS−PAGE (Mini-PROTEAN II system, Bio-Rad Laboratories), and gel electrophoresis was conducted at 200 V at 4 °C. Bands were visualized using the Molecular Dynamics PhosphorImager system.

Assay for MutY Activity. Reaction mixtures (10 μL) containing 20 nM appropriate ^{32}P-labeled duplex and varying amounts of MutY were incubated at 37 °C for 5 min in a standard MutY buffer (50 mM Tris-HCl, pH 7.5, 100 mM KCl, 5 mM EDTA). In experiments measuring pH dependence, 25 mM sodium phosphate, adjusted to the appropriate pH, was substituted for Tris-HCl. Reactions were terminated by addition of 2.5 μL of 0.5 M putrescine-HCl, pH 8.0, followed by heating for 5 or 30 min at 95 °C. Formamide dye loading buffer (6.25 μL) was added, and aliquots were analyzed by 20% PAGE with 7.2 M urea. For measurements of intrinsic AP lyase activity, reactions were terminated by adding 5 μL of formamide dye loading buffer and cooling in an ice bath or heating at 95 °C for 1 or 5 min. Reaction products in gels were quantified using the PhosphorImager system.

Mutagenesis Assay. Single colonies of *E. coli* CC104 *mutY* (*32*) transformed with various forms of *mutY* on pET13a were inoculated into LB medium containing 25 μg/mL kanamycin and 25 μg/mL tetracycline. The culture was grown overnight with shaking at 37 °C. From each culture, 0.1 mL was removed and plated onto rifampicin−kanamycin−tetracycline LB plates to score for Rif^r mutants; also, 0.1 mL of a 10^{-6} dilution was plated onto kanamycin−tetracycline LB plates to quantify viable cells. The number of colonies was determined after overnight incubation at 37 °C (*33*).

The rate of appearance of colonies resistant to rifampicin was determined as previously described (*33*). Data were analyzed by F-test; the data sets that produced the value of $P > 0.01$ were reanalyzed by two-tailed heteroscedastic *t*-test. Statistical analysis was performed using a package from Microsoft Excel 97 SR-1 software. From all pairwise comparisons, values of $P > 0.01$ in the F-test were produced only in pairs "*mutY* vs *mutY* + pET13a MutY K142Q" and "*mutY* + pET13a MutY vs *mutY* + pET13a MutY K142Q", and $P > 0.01$ in the *t*-test only in the pair "*mutY* + pET13a MutY vs *mutY* + pET13a MutY K142Q".

Gel Mobility Shift Assay. Reaction mixtures (10 μL) containing 50 pM ^{32}P-labeled appropriate duplex and various amounts of MutY were incubated at 4 °C for 1 h in a standard MutY buffer supplemented with 10% glycerol. In experiments measuring pH dependence, 25 mM sodium phosphate, adjusted to the appropriate pH, was substituted for Tris-HCl. Aliquots (4 μL) were loaded directly onto 8% nondenaturing PAGE (17 cm long) gels, prerun in 0.5× TBE at 300 V for at least 2 h. Loading was done at 300 V, a tracer dye (bromophenol blue, 0.5× TBE, 10% glycerol) was loaded in a separate lane. After 15 min, voltage was reduced to 190 V, and electrophoresis was continued for 2 h. Bands were quantified as described above. Binding constants were calculated from three independent experiments using a Jandel SigmaPlot v5.00 nonlinear fit routine.

Active Site Titration and Single Turnover Experiments. Experiments were performed as described (*34*), except that concentrations of MutY in the active site titration experiments were 1, 2, and 4 nM, and the buffers were as described above. Time points in these experiments were 2, 4, 6, and 8 min, and in single turnover experiments were 0.25, 0.5, 1, 2, 3, 5, 10, 20, and 30 min. Kinetic parameters were calculated from three independent experiments using a Jandel SigmaPlot v5.00 nonlinear fit routine.

Protein Crystallization. Single crystals of the MutY p25 K142Q mutant were obtained using the hanging drop vapor diffusion method by mixing 5 μL of freshly purified protein solution (2 mg/mL protein, 50 mM HEPES-KOH, pH 8.0, 400 mM NaCl) with an equal volume of reservoir solution (1.4−1.8 M $LiSO_4$, 50 mM HEPES-KOH, pH 8.0−8.5, 400 mM NaCl, 50 mM $MgSO_4$). The mixed drops (10 μL) were suspended over 1 mL of reservoir solution at 15 °C using 6×4 Linbro tissue culture plates.

Crystallographic Data Measurements. Crystals of MutY p25 K142Q were flash-cooled to 100 K under a stream of liquid nitrogen after soaking for approximately 3 min in a solution containing 78% crystallization solution and 22% glycerol. A complete diffraction data set at 1.35-Å resolution was measured on a single crystal of MutY p25 K142Q using a Quantum-4 CCD area detector (ADSC) at the X26C beamline, National Synchrotron Light Source facility, Brookhaven National Laboratory (Upton, NY). All diffraction data were processed with the DENZO and SCALEPACK software (*35*) to give a final merged intensity data set that was then used for model building and refinement.

Model Building and Refinement. Since the crystals of MutY p25 K142Q were completely isomorphous to the crystals of wild-type MutY p25 (*C*2 space group and less than 2% difference in the unit cell dimensions), we used the 1.4-Å resolution structure of wild-type MutY p25 (*18*; PDB entry 1MUY) as an initial solvent-free model. The position of the protein in the unit cell was initially improved by rigid body refinement. Difference Fourier calculations were used to locate all solvent molecules, as well as to determine conformational changes in the active site and elsewhere in the protein. Subsequent refinement was performed using alternating rounds of manual rebuilding and simulated annealing or positional minimization with individual temperature factor refinement. Crystallographic refinement was performed using the CNS software package (*36*). Ten percent of the measured reflections were set aside throughout all refinement steps and used to calculate the R_{free} value (*37*). All model building was done with the O software package (*38*). Solvent molecules were included gradually from (F_o-F_c) electron density maps if the peak height was stronger than 3.5 σ and its position was between 2.5 and 3.5 Å relative to a suitable hydrogen bond donor or acceptor. In addition to manual inspection, geometry evaluation, and difference density minimization, progress of the refinement was confirmed by the steady decrease in values for R and R_{free}. The figures presented in this paper were prepared using the MOLSCRIPT and BOBSCRIPT software (*39*).

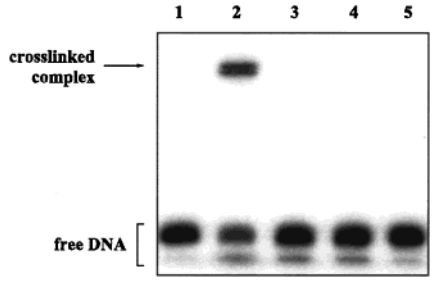

FIGURE 1: Cross-linking of wild-type MutY and K142 mutants to DNA containing dA:8-oxodG. Cross-linking was performed with sodium borohydride as described under Experimental Procedure. Lane 1, no enzyme; lane 2, wild-type MutY; lane 3, MutY K142A; lane 4, MutY K142Q; lane 5, MutY K142R. The amount of protein in the reaction was 30 ng.

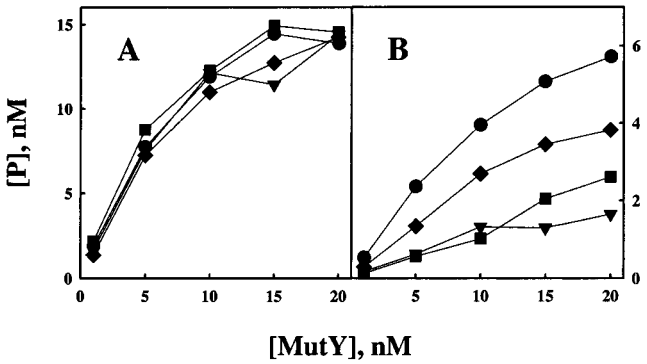

FIGURE 2: Activity of MutY proteins on substrates containing dA:8-oxodG and dA:dG. Panel A, dA:8-oxodG; panel B, dA:dG. Circles, wild-type MutY; triangles, MutY K142A; squares, MutY K142Q; diamonds, MutY K142R. Assay was performed as described under Experimental Procedures.

RESULTS

MutY K142 Mutants Do Not Form a Schiff Base with DNA. Lys-142 in MutY forms a cross-link with substrate DNA following reduction with sodium borohydride (*23*). On the basis of models of MutY complexed with its DNA substrate (*23*) and X-ray crystallographic analyses of MutY p25 (*18*), Lys-142 is predicted to be positioned within approximately 3.5 Å of C1′ in the target adenine. To show that mutants at position 142 are unable to form a Schiff base, we performed sodium borohydride reduction with recombinant purified MutY wild-type, K142A, K142Q, and K142R proteins and a dA:8-oxodG DNA substrate. All mutant proteins were devoid of Schiff base-forming activity, showing less than 2% of the cross-linking activity of the wild-type MutY when used in 4-fold molar excess (Figure 1). The residual cross-linking may be due to wild-type MutY that copurified with mutant proteins from the *E. coli* expression strain.

Catalytic Activity and Substrate Specificity of MutY K142 Mutants. The activities of MutY wild-type, K142A, K142Q, and K142R were compared using dA:8-oxodG and dA:dG substrates. As shown in Figure 2, panel A, none of the K142 mutations affected the ability of MutY to excise adenine from dA:8-oxodG mispairs. However, clear differences were observed when dA:dG was used as substrate. MutY K142A and K142Q displayed greatly reduced activity toward this substrate as compared to the wild-type enzyme; K142R was affected but to a lesser degree (Figure 2, panel B).

To investigate whether K142 mutations influenced lesion processing following the glycosylase step, we performed the reaction under controlled thermal conditions to minimize nonenzymatic AP site cleavage. Neither wild-type nor mutant MutY possessed detectable AP lyase activity when tested with either the dA:8-oxodG or dA:dG substrate (wild-type MutY is compared to MutY K142Q in Figure 3). We observed moderate cleavage of substrates containing an abasic site opposite dG or 8-oxodG with MutY K142A. Cleavage did not decrease when an excess of unlabeled competitor carba-dA:8-oxodG duplex was introduced to the reaction but was readily outcompeted with dA:T and 8-oxo-carba-dG:dC duplexes (data not shown). Thus, the observed cleavage is most likely due to Fpg or endonuclease VIII contaminating the MutY K142A preparation. Our observations do not support the claim (*40*) that MutY K142A is an AP lyase and can induce δ elimination at preformed AP sites.

On the basis of results of the experiments described above, MutY K142Q was selected for a more detailed investigation based on the following reasons: (i) in this mutant, a positively charged lysine is replaced with an amino acid which is neutral but polar and similar to lysine in side chain bulkiness; (ii) it was the easiest mutant to purify in sufficient quantities; (iii) its activity on a dA:dG substrate was decreased to the same extent as for MutY K142A; and (iv) the activity was not complicated by the presence of other AP lyases.

MutY K142Q Complements the mutY Mutator Phenotype in vivo. The ability of MutY K142Q to reduce the rate of spontaneous mutations in *mutY E. coli* CC104 was determined using the rifampicin resistance assay (*33*). Results are summarized in Table 1. Disruption of the chromosomal *mutY* gene resulted in a 72-fold increase in the rate of appearance of Rif^r colonies ($P < 0.001$). *MutY* bacteria were transformed with an overexpressing pET13a plasmid carrying wild-type MutY or MutY K142Q. Although expression in the pET family of vectors is under control of the T7 promoter, basal transcription still occurs due to low-level read-through activity of bacterial RNA polymerase (*41*). When wild-type MutY or MutY K142Q were introduced into *mutY* cells, the rate of appearance of Rif^r colonies decreased 12−20-fold ($P < 0.01$), remaining slightly higher than in wild-type *E. coli*. There was no statistically significant difference between wild-type MutY and MutY K142Q rescue constructs ($P = 0.25$ by F-test, $P = 0.55$ by *t*-test). Interestingly, transformation using the empty pET13a plasmid caused a further increase in mutation rate (14-fold, $P < 0.001$). This observation may explain why the elevated mutation frequency of the MutY-expressing vector could not be decreased to wild-type levels. Similar effects have been observed with other pET family vectors (*42*). We conclude that MutY K142Q can suppress spontaneous mutagenesis in *mutY E. coli* with an efficiency comparable to wild-type MutY.

Affinity of Wild-Type MutY and MutY K142Q for Substrate and Reaction Intermediate Analogues. To determine more precisely the mechanism responsible for the decrease in activity against dA:dG mispairs observed with MutY K142Q, we used a gel mobility shift assay to compare binding of selectively modified DNA by wild-type and mutant MutY. Since the kinetics of association and dissociation events are complex and the observed values for K_D reflect binding of enzyme to both substrate and product (*23*, *43*−*45*), we utilized a carbocyclic analogue of adenine, carba-dA (*28*), and a tetrahydrofuran analogue of an abasic site, F (*29*),

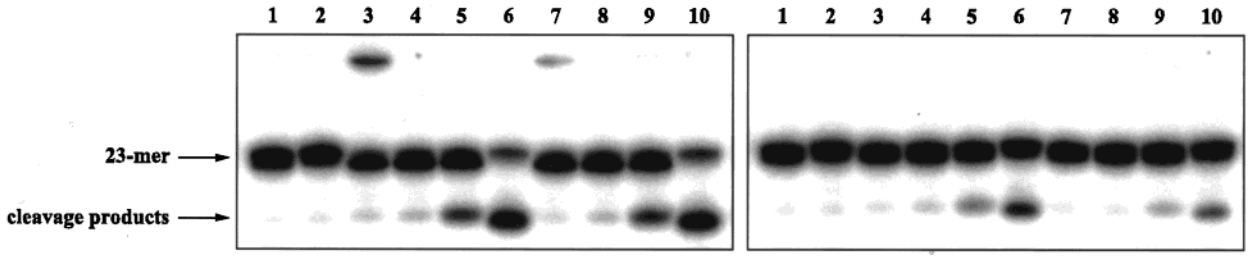

FIGURE 3: Products of wild-type MutY and MutY K142Q acting on substrates containing dA:8-oxodG and dA:dG. Left panel, dA:8-oxodG; right panel, dA:dG. Lanes 1 and 2, no protein; lanes 3−6, wild-type MutY; lanes 7−10, MutY K142Q. Reactions were performed under standard assay conditions (see Experimental Procedures) with 20 nM MutY. After the reaction was complete, products were treated as follows: lanes 1, 5, and 9: heated for 5 min at 95 °C; lanes 2, 6, 10: 100 mM putrescine-HCl added, heated for 30 min at 95°; lanes 3, 7: held on ice; lanes 4, 8: heated for 1 min at 95 °C.

Table 1: Suppression of *mutY* Mutator Phenotype by Wild-Type MutY and MutY K142Q

genomic *mutY*	transforming plasmid	Rif^{r}colonies/10^8 cells[a]
wild type	none	0.67 ± 0.51
mutY::mini-*tet*	none	49 ± 19
mutY::mini-*tet*	pET13a	680 ± 330
mutY::mini-*tet*	pET13a MutY	2.3 ± 2.7
mutY::mini-*tet*	pET13a MutY K142Q	4.0 ± 5.0

[a] Expressed as the average ± standard deviation.

Table 2: Binding of Wild-Type MutY and MutY K142Q to DNA Using Uncleavable Substrate Analogs

			K_D, nM[a]	
duplex	buffer	pH	MutY	MutY K142Q
carba-dA:dG	Tris-HCl	7.5	21.8 ± 4.3	298 ± 44
	phosphate	7.5	27.2 ± 4.5	165 ± 30
	phosphate	5.7	21.4 ± 3.9	38.8 ± 8.8
carba-dA:8-oxo-dG	Tris-HCl	7.5	0.316 ± 0.099	0.527 ± 0.130
F:dG	Tris-HCl	7.5	0.568 ± 0.163	0.502 ± 0.134
F:8-oxo-dG	Tris-HCl	7.5	0.014 ± 0.008	0.017 ± 0.005

[a] Expressed as the estimated regression coefficient ± standard error.

which structurally mimic substrate and product, respectively, but cannot be processed by MutY (*15*). The concentration of enzyme capable of binding the ligand was determined first in titration experiments, using F:8-oxodG as ligand. The fraction of active enzyme was 47.5% for wild-type MutY and 50.2% for MutY K142Q. Concentrations of enzymes used in the gel mobility shift assay were corrected using these coefficients.

Results of these experiments are shown in Table 2. MutY K142Q was identical to wild-type MutY in terms of its ability to bind carba-dA:8-oxodG, F:dG, and F:8-oxodG. However, the K_D for carba-dA:dG was 6−14-fold higher for MutY K142Q than for wild-type MutY. This observation suggests that Lys-142 is important for binding dA:dG mispairs but not dA:8-oxodG or substituents containing the abasic site. Thus, mutation at Lys-142 appears to lead to a decrease in dA:dG processing through a decrease in the intrinsic affinity of MutY for this mispair.

Catalytic Efficiency of Wild-Type MutY and MutY K142Q in Single Turnover Experiments. To determine whether the K142Q mutation affected a catalytic step in MutY-dependent base release, we conducted single turnover experiments with dA:dG as substrate. Both MutY forms were analyzed in active site titration experiments using dA:8-oxodG as substrate to determine the concentration of the active species. The time course of MutY K142Q action indicated very slow product release, similar to the wild-type enzyme (data not shown). The fraction of active species was 90.5% for wild-type MutY and 63.6% for MutY K142Q with fresh protein. Specific activity decreased slowly over time (21.7 and 15.1%, respectively, after 4 months storage at −20 °C); however, the measured kinetic constants were not significantly affected if the active species concentrations were identical. The concentration of enzymes used in single turnover experiments was corrected using these coefficients. The observed k value, k_{obs}, for dA:dG was 0.173 ± 0.004 min^{-1} for wild-type MutY and 0.096 ± 0.003 min^{-1} for MutY K142Q (Figure 4, panel A, Table 3). However, if we assume that the true values of K_D for dA:dG are close to those for carba-dA:dG, the condition $[E_0] \gg K_D$ is not valid for MutY K142Q, i.e., $[E_0] = 100$ nM, and the true value for k_2 (a catalytic constant for the glycosidic bond cleavage) will be given by the equation $k_2 = k_{obs}(K_D + [E_0])/[E_0]$. Using this equation and K_D values determined for carba-dA:8-oxodG, k_2 is estimated as 0.211 ± 0.010 min^{-1} for wild-type MutY and 0.382 ± 0.090 min^{-1} for MutY K142Q. We conclude that the catalytic step does not contribute to the observed decrease in MutY K142Q activity against dA:dG mispairs, leaving effects on K_D as the major factor.

Dependence of Wild-Type MutY and MutY K142Q Activity on pH. The reduced activity of MutY K142Q on dA:dG-containing substrates suggested that Lys-142 might be involved in distinguishing between the syn and anti conformations of the nucleoside opposite dA. At neutral pH, the dA:8-oxodG mispair exists as dA(anti):8-oxodG(syn) (*46*, *47*), while dA:dG is dA(anti):dG(anti) (*48*, *49*). At lower pH values, the dA:dG pair becomes dA(anti):dG(syn) ($pK_a = 6.0$) due to protonation of adenine at N1, enabling it to form a hydrogen bond to the N7 of guanine (*49*). At acidic pH, MutY has increased activity on dA:dG, while its activity on dA:8-oxodG is pH-independent (*15*). If the K142Q mutant is unable to recognize the nucleotide opposite dA in the anti conformation, its activity should resemble that of wild-type MutY at lower pH. The experiment shown in Figure 5 shows this to be the case. The ratio of activity of MutY K142Q to wild-type MutY was about 0.2 at pH 7.2−7.5 but increased to 0.8−1.0 at pH 5.7 (lowest pH tested) to 6.1. Both forms of MutY behaved similarly over the pH range tested. At pH 5.7−6.1, the activity was essentially pH-independent, then dropped almost linearly. Both wild-type MutY and MutY K142Q cleaved the dA:8-oxodG-containing substrate in a pH-independent manner over the range of pH 5.7−7.5 (data not shown).

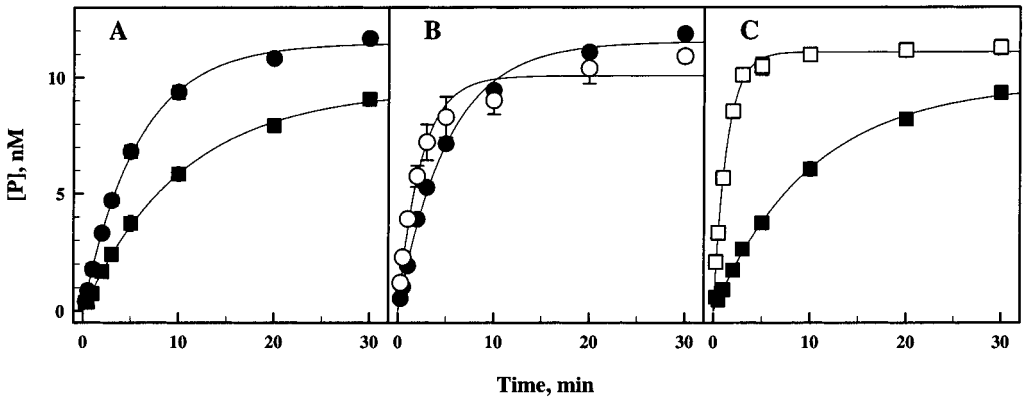

FIGURE 4: Single turnover kinetics of wild-type MutY and MutY K142Q. Kinetic experiments were performed as described under Experimental Procedures. Circles denote wild-type MutY, squares, MutY K142Q. Filled symbols represent pH 7.5, open symbols, pH 5.7. Panel A: wild-type MutY and MutY K142Q in Tris-HCl, pH 7.5; panel B: wild-type MutY in phosphate buffer at pH 5.7 and 7.5; panel C, same as panel B using MutY K142Q. Error bars represent standard deviations in data from three independent experiments.

Table 3: Catalytic Constants for Wild-Type MutY and MutY K142Q[a]

MutY	buffer	pH	k_{obs}, min^{-1}	k_2 calc, min^{-1}
wild type	Tris-HCl	7.5	0.173 ± 0.004	0.211 ± 0.010
	phosphate	7.5	0.192 ± 0.006	0.244 ± 0.013
	phosphate	5.7	0.421 ± 0.031	0.512 ± 0.043
K142Q	Tris-HCl	7.5	0.096 ± 0.003	0.382 ± 0.090
	phosphate	7.5	0.098 ± 0.003	0.259 ± 0.054
	phosphate	5.7	0.736 ± 0.019	1.02 ± 0.10

[a] Expressed as the estimated regression coefficient ± standard error.

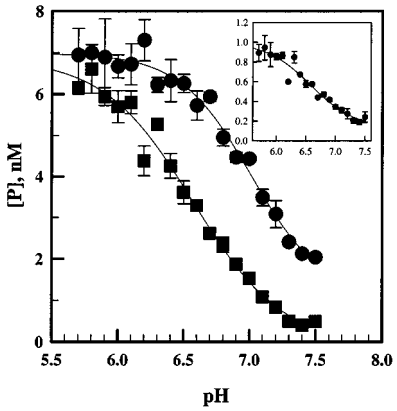

FIGURE 5: pH dependence of MutY activity. Reactions performed under standard conditions (see Experimental Procedures) with 20 nM MutY. Filled circles, wild-type MutY; open circles, MutY K142Q. Inset: ratio of activity between MutY K142Q and wild-type enzyme plotted vs pH. Error bars represent standard deviations in data from three independent experiments.

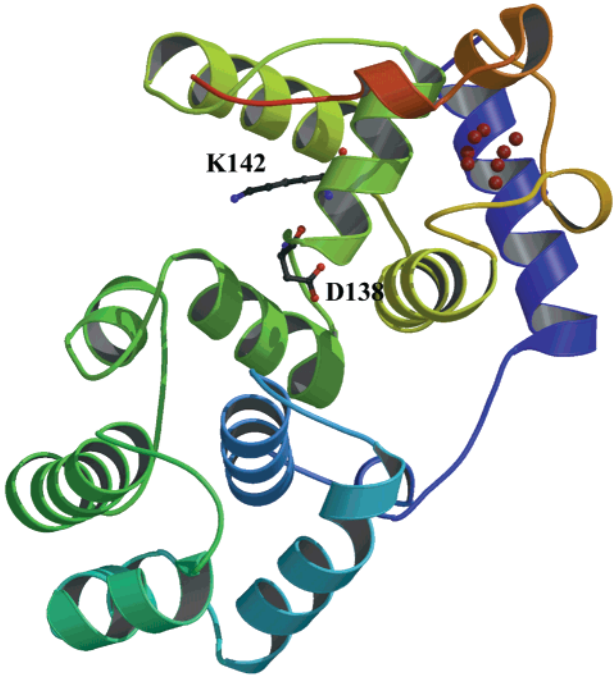

FIGURE 6: Ribbon diagram of MutY p25 domain. The diagram showing the overall structure of MutY p25 and its secondary structure elements is based on coordinates reported by Guan et al. (*18*), PDB access number 1MUY. The polypeptide chain is color-coded with the N-terminus in dark blue, C-terminus in red and gradiated colors in between. Atoms forming the $[Fe-S]_4$ cluster are shown as red spheres. Note the wide groove at the center of the molecule, where Asp-138 and Lys-142 are located.

To determine which step in the MutY-catalyzed reaction was affected by changing pH, we measured the dissociation constant and k_2 values at the extremes of the pH range studied, pH 5.7 and 7.5. The decrease in pH dramatically increased binding of MutY K142Q to carba-dA:dG, bringing the value close to that for the wild-type enzyme (Table 2). In contrast, binding of wild-type MutY was influenced very little by pH (Table 2). Catalytic constants were determined from single turnover experiments, and the values recorded were corrected for differences in K_D as described above. Unlike the binding constant, which improved for MutY K142Q only, calculated values for k_2 for wild type and K142Q enzymes were affected by the decrease in pH (Figure 4, panels B and C, Table 3). MutY K142Q was stimulated somewhat more significantly (2.1-fold increase in k_2 for wild-type MutY vs 3.9-fold for MutY K142Q). We conclude that the effect of pH on MutY K142Q is mostly due to an increase in affinity of the mutant protein for the substrate, possibly due to a transition of 8-oxodG from syn to anti conformation.

Three-Dimensional Structure of Wild-Type MutY and MutY K142Q Catalytic Domains. The recently reported structure of native MutY p25 (*18*) shows a deep and wide groove in the center of the protein that is well-suited for binding DNA. Lys-142 is located in this region, and the side chain of this residue extends into the center of the groove (Figure 6). A detailed structural analysis of the MutY p25 K142Q mutant was performed to examine potential conformational changes that might explain the altered properties of the mutated

Table 4: Parameters for Crystal Structure Analysis of MutY p25 K142Q

Data Collection	
beamline	NSLS/X26C
detector	Q4-CCD
wavelength (Å)	1.10
space group	*C*2
unit cell dimensions (Å)	$a = 83.49$ $b = 50.12$ $c = 70.38$ $\beta = 122.68°$
total no. of reflections	217 600
reflections above 1σ	215 765
unique reflections	49 330
resolution limit (Å)	1.35
completeness (last shell) (%)	91.7 (55.4)
redundancy	4−5
$\langle I/\sigma(I)\rangle$	13.5
R_{sym} (last shell)[a] (%)	6.2 (21.4)
Refinement	
resolution range (Å)	40.0−1.35
no. of protein atoms[b]	1770
no. of solvent molecules[c]	271
B_{ave}	11.1
R value (%)	16.4
R_{free}[d] (%)	18.2
rmsd for bond lengths[e] (Å)	0.017
rmsd for bond angles[e] (deg)	1.6

[a] R_{sym} is the unweighted *R* value on *I* between symmetry mates. [b] Including $[Fe-S]_4$ cluster. [c] Not including 4 glycerol molecules and 1 sulfate anion. [d] R_{free} is *R* value for 10% of reflections against which the model was not refined. [e] R.m.s. deviation from ideal stereochemistry.

enzyme. Crystals began to form after 1−2 days (yellow, sharp edges and faces) and grew to full size (typically 0.3×0.1×0.05 mm) within 4−5 days. Representative measurement and refinement parameters are shown in Table 4. Diffraction patterns obtained indicate that these crystals belong to the monoclinic space group *C*2 with unit cell dimensions of $a = 83.5$ Å, $b = 50.1$ Å, $c = 70.38$ Å and $\beta = 122.68°$, with one protein molecule in the asymmetric unit. As such, they appear completely isomorphous to the reported crystals of the MutY p25 (*18*). The resulting difference maps were very clear and enabled a straightforward interpretation and model building. Four glycerol molecules, originating from the 22% glycerol solution used for premounting cryosoaking, and a sulfate anion, originating from the lithium sulfate of the crystallization solution, were found in the final cycles of refinement and model building. The final MutY p25 K142Q model contains 1770 protein atoms and 271 ordered solvent molecules. None of the amino acid residues of the final model are in disallowed regions of the Ramachandran plot, and 91.7% of them are found in the most favored region. As in the wild-type structure, a *cis*-peptide bond was found between Tyr-219 and Pro-220. The difference density confirmed full replacement of the lysine residue by glutamine at position 142 (Figure 7). No major conformational changes were observed as a result of the K142Q mutation relative to the wild-type structure except for the mutated residue and its immediate environment.

A least-squares fit of the two structures (wild type vs K142Q) results in an rms difference between all C_α atoms of the two models of 0.536 Å. This value indicates a small, but significant difference, reflecting local conformational changes of surface side chains. These may originate from the slightly different crystallization conditions used for the two enzymes. Most of the deviating residues (e.g., Arg-19)

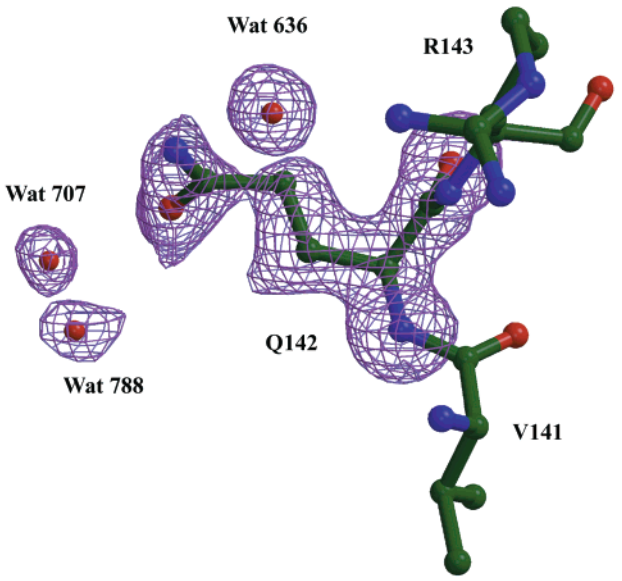

FIGURE 7: Electron density difference map (F_o-F_c coefficients) for the final structure of MutY p25 K142Q at 1.35 Å resolution. The observed "omit" density (contour level of 4σ, blue) for Gln-142 and its three neighboring water molecules is shown.

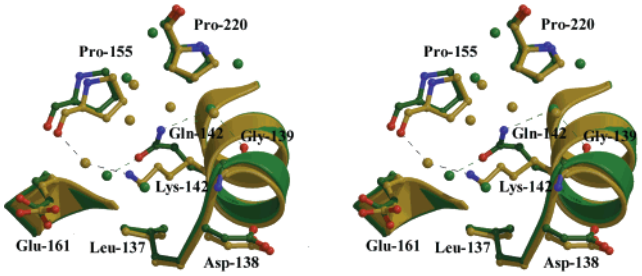

FIGURE 8: Stereoview comparing the regions surrounding residue 142 in the refined structures of MutY p25 and MutY p25 K142Q. Spheres of 6 Å radius are shown; MutY p25 is in yellow (1.40 Å resolution); MutY p25 K142Q is in green (1.35 Å resolution). Nitrogen atoms of side chains are labeled in blue, and oxygen atoms are in red. Note the different orientations of Lys-142 in MutY p25 and Gln-142 in MutY p25 K142Q and the hydrogen bonding interactions in which these residues are involved.

are located on helices and loops facing the DNA binding cleft; it seems unlikely that these randomly oriented conformational changes are responsible for the altered biochemical properties of MutY K142Q.

Examining the region around residue 142, one finds differences both in the local conformation of the side chains as well as in the arrangement of water molecules bound in the vicinity of this site (Figure 8). The glutamine side chain in the K142Q mutant extends in a different direction in the binding groove, a result of its different length, conformation, and functional groups, as compared to lysine. The two residues also form different networks of hydrogen bonds. The terminal amine group of lysine forms a hydrogen bond with two water molecules, W1201 (3.14 Å) and W1159 (2.92 Å). W1201 is hydrogen bonded to another water (W1059, 2.76 Å), while W1159 is additionally hydrogen bonded to the backbone carbonyl group of Pro-155 (2.43 Å), located on a nearby α-helix on the other side of the DNA binding cleft. In contrast, the glutamine amide group makes a hydrogen bond to a water molecule, W636 (3.11 Å), which also is hydrogen bonded to the backbone carbonyl group of Gly-139 (2.91 Å) located on the same α-helix as Gln-142.

The terminal carbonyl group of Gln-142 makes a hydrogen bond to a single water molecule (W707, 2.67 Å). These hydrogen bonding networks are shown in Figure 8 where the water-bridged interaction between Lys-142 and Pro-155 in wild-type MutY p25 pulls Pro-155 (and the helix of which it is an integral part) closer to Lys-142, as compared to the K142Q mutant where this interaction is missing. These interactions narrow the DNA groove in the wild-type protein as compared to the K142Q mutant. Nevertheless, as discussed below, none of the local structural changes is likely to be responsible for the significant difference in biochemical properties of the two MutY variants.

DISCUSSION

Lys-142 of *E. coli* MutY has been identified as a nucleophilic group participating in Schiff base formation between the enzyme and C1′ of the target dA (*23*, *40*). Since MutY behaves generally as a monofunctional glycosylase (*23*, *24*), the functional role of Schiff base formation is unclear. Recently, David and colleagues showed that when Lys-142 is mutated to alanine, MutY retains its activity on dA:8-oxodG-containing substrates and is able to reduce mutagenesis in vivo (*26*). However, Lys-142 by itself or by means of Schiff base formation might be required for events not directly involved in the chemical step of catalysis, such as substrate discrimination, regulation of product release, or protein−protein interactions.

We conducted a series of experiments aimed at elucidating the role of Lys-142 in the action of MutY by replacing this residue with alanine, glutamine, or arginine and investigating the biochemical properties of the resulting mutants. As expected, mutant proteins were unable to form cross-links with substrates containing dA:8-oxodG mispairs. Nevertheless, they retained full activity in excising adenine from dA:8-oxodG mispairs and one of them, MutY K142Q, complemented the *mutY* mutator phenotype of *E. coli* in a rifampicin resistance assay and showed a reaction mechanism involving a slow product release step, also observed in wild-type MutY (*23*). However, when activities of wild type and mutant MutY proteins were compared using substrates containing a dA:dG mispair, K142A and K142Q mutations significantly impaired the enzyme's ability to remove adenine from DNA. In the case of MutY K142Q, this impairment proved to be due to a marked decrease in the affinity of the enzyme for the dA:dG-containing substrate. In contrast, the affinity of MutY K142Q for substrates containing 8-oxodG and for abasic site analogues opposite either dG or 8-oxodG was comparable to wild-type protein.

Wild-type MutY is more active on DNA containing dA:8-oxodG than on duplexes containing dA:dG (*15*, *34*). Mechanisms explaining the ability of MutY to discriminate between dG and 8-oxodG in the noncleaved strand have focused largely on the role of the C-terminal (p14) domain (*50*, *51*). Removal of the p14 domain reduces the ability of MutY to bind DNA and to form a Schiff base with substrates containing adenine or an abasic site positioned opposite 8-oxodG. Processing of dA:dG mispairs is largely unaffected (*44*, *51*). The p14 domain demonstrates limited sequence homology but significant structural resemblance to MutT, an 8-oxodGTPase/8-oxoGTPase (*44*, *52*), and may represent a universal 8-oxoG binding domain.

Discrimination between dG and 8-oxodG also can be explained by conformational analysis of the DNA substrate. A detailed study of substrate specificity suggested that specific binding of MutY was conferred by its interaction with a unique configuration of hydrogen bond acceptors and donors displayed in the major groove of DNA (*15*). This configuration is present when dG(syn) pairs to dA(anti). The dA:8-oxodG pair assumes this conformation naturally, driven by steric interference by the C8 substituent (*53*) and stabilization by a Hoogstein base pair (*46*, *47*). At physiological pH, the dA:dG pair tends to assume an anti−anti conformation (*48*, *49*). However, at pH values below 6.0, dG is mainly in the syn conformation, and the activity of MutY on this mispair significantly increases (*15*). The increased activity could reflect ionization of a critical functional group of the enzyme, easier removal of adenine following protonation, or improved substrate recognition or binding. In the present study, we determined K_D by gel retardation assay and k_2 by single turnover experiments and showed that the increased activity of wild-type MutY on the dA:dG mispair at lower pH is due to increased efficiency of the catalytic step rather than increased substrate affinity.

Our finding that MutY K142A and K142Q mutants do not efficiently remove adenine from dA:dG mispairs at pH 7.5 suggests that the conformational change in the substrate is an active process in which Lys-142 is directly involved. In contrast to wild-type MutY, decreasing pH is associated with increased binding and improved catalytic constant for the mutant protein. The proposed mechanism of substrate recognition by MutY is illustrated in Figure 9. Wild-type MutY binds dA(anti):8-oxodG(syn) or dA(anti):dG(syn) with high affinity. When the enzyme encounters dA(anti):dG(anti), it employs Lys-142 to assist deoxyguanosine in adopting a syn conformation, stabilizing this nucleoside in the enzyme−DNA complex. The effect of pH on k_2 probably is not related to Lys-142 since (i) it is observed in both wild-type and mutant MutY and (ii) conformational change of deoxyguanosine can be affected solely by protonation of adenine (*49*), while in the enzyme−substrate complex adenine is flipped out of the helix into a recognition pocket and thereby separated from the opposite base. Thus, the effect of pH on k_2 may reflect ionization of a critical amino acid near the catalytic site or protonation of adenine, creating a better leaving group.

A change in the three-dimensional structure of the enzyme was considered as one of several possible explanations for the altered properties of MutY K142Q. Such a change might have been anticipated on the basis of the native structure, since Lys-142 participates in an important interaction involving neighboring α-helixes, both of which are part of the elongated binding region for the DNA duplex. The tight packing of these two helixes could be significantly altered by the absence of this interaction and hence affect the overall structure of the enzyme and its binding to DNA. The side chain of glutamine is one carbon shorter than of lysine, and these two side chains carry terminal functional groups with different hydrogen-bonding properties: the free amino group of lysine can only be a hydrogen bond donor while the amide group of glutamine can be both donor and acceptor.

The observed differences between the three-dimensional structures of wild-type MutY and MutY K142Q are relatively small. There is no global change in the overall structure of

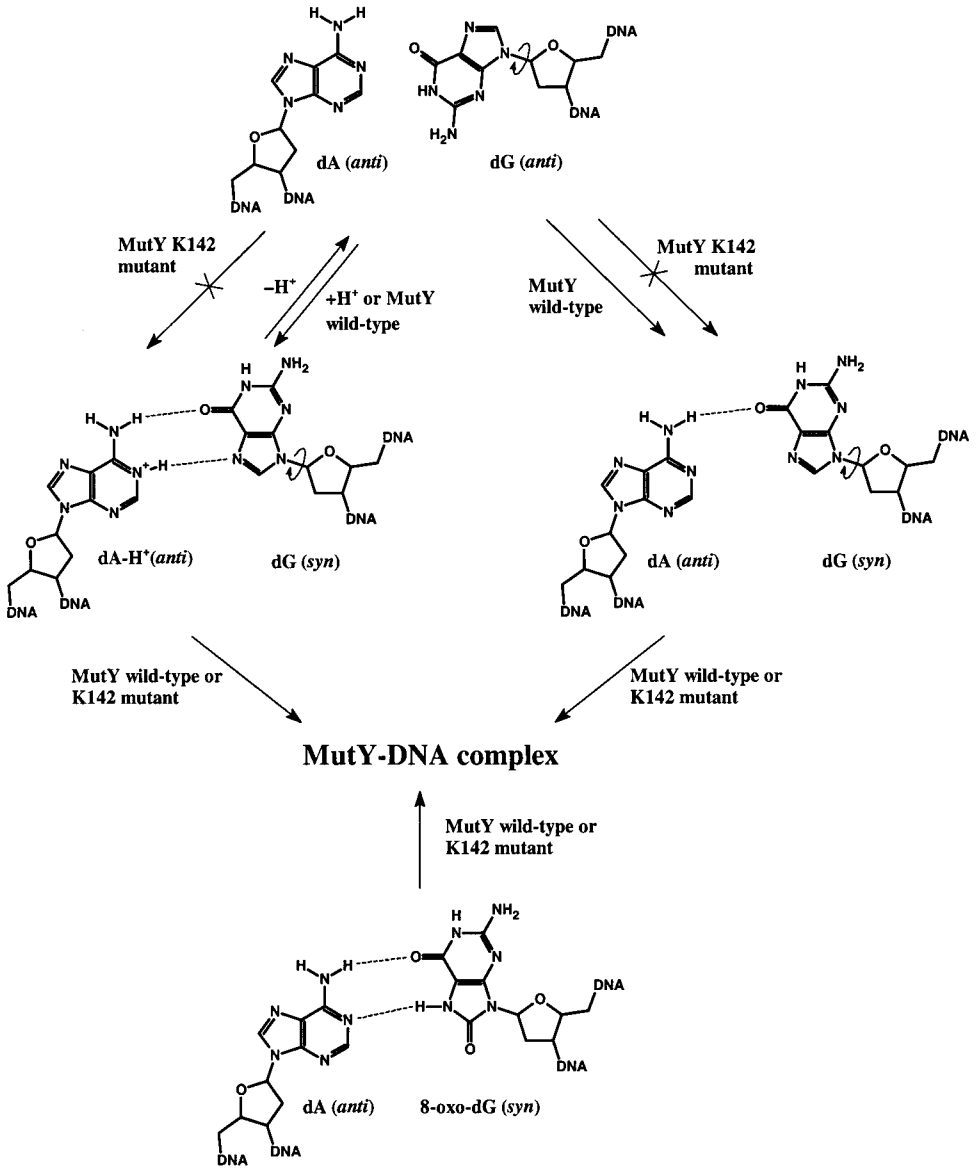

FIGURE 9: Scheme for substrate recognition by MutY. The dA(anti):dG(anti) mispair must be converted into dA(anti):dG(syn) before productive binding by MutY. Acidic pH promotes this process by protonating N1 of adenine. Wild-type MutY employs Lys-142 to assist the conversion, with or without N1 protonation. MutY K142Q is unable to convert dG(anti) to dG(syn) and binds the dA:dG mispair poorly at neutral pH. The dA:8-oxodG mispair exists as dA(anti):8-oxodG(syn) and is efficiently bound by both wild-type and K142Q MutY.

the enzyme as a result of the K142Q mutation, indicating that Lys-142 is less critical than expected in determining overall enzyme conformation and intramolecular helix−helix packing. The small rms deviations between the two structures mainly reflect alternative conformations of amino acid side chains on the surface of the protein. Importantly, the size and overall shape of the DNA binding groove of the two MutY p25 variants remains essentially unchanged. Conformations and hydrogen bond patterns are affected by buffer conditions and may adjust further after the DNA is bound in the active site. It is therefore unlikely that the small surface conformational changes observed between the two MutY variants could account for different biochemical properties of the two proteins.

Alternative explanations for the functional differences between the wild-type and K142Q enzymes may reflect the different chemical nature of the two side chains and the slightly different position of their functional group within the DNA binding groove. If Lys-142 participates in critical enzyme−DNA interactions, they could potentially be affected by the K142Q mutation, even if the overall structure of the enzyme and the shape of its DNA binding groove are unchanged. In such a case, the properties of MutY K142Q could be accounted for by the shorter side chain of glutamine, its different orientation in the DNA binding site (see Figure 8), and the different hydrogen bonding properties of the amide and amino groups. It is interesting to note that in MutY K142R, where a positive charge at position 142 is still present, the activity on a dA:dG substrate is not as significantly affected as in MutY K142A and K142Q (Figure 2), indicating that electrostatic interactions may be important for Lys-142 function.

Our results suggest that Lys-142 makes direct contact with deoxyguanosine in a dA:dG mismatch. This conclusion is in agreement with a report that Lys-142 of MutY can be cross-linked to C5 of 8-oxoG via one-electron oxidation by Na_2IrCl_6 (*54*). At the same time, Lys-142 was shown to form a Schiff base with C1′ of deoxyadenosine when in complex

with substrate DNA duplex (*23*, *26*, *40)*. However, considering the structures of wild-type MutY p25 and MutY p25 K142Q, it is difficult to model a DNA duplex in the active site of the enzyme (assuming extrahelical adenine without gross distortion of the enzyme upon binding DNA) in such a way that Lys-142 can react with both sites when MutY is bound to DNA. One possible explanation for our experimental data is that the enzyme binds DNA in more than one mode and that one of these modes accounts for the K142-guanine interaction, while a different mode accounts for the K142-adenine interaction. Elucidating the nature of such binding modes would be of great interest. They may be dynamic—for example, one existing at the stage of mismatch recognition, the other immediately before catalysis—or static, if the enzyme in some cases bound in an opposite orientation and inserted guanine rather than adenine into the active site pocket.

The p14 domain of MutY is postulated to be in direct contact with 8-oxodG (*44*). As seen from the three-dimensional structure (*18*, *52*, this study), Lys-142 is situated in the vicinity of the C-terminus of p25, projecting approximately in the same direction (Figure 6). Thus, structural data are consistent with a model in which both Lys-142 and p14 contact the nucleoside opposite dA. Their functions in substrate recognition may be complementary; for example, p14 may ensure efficient binding of 8-oxodG-containing substrates, while Lys-142 is necessary for binding the dA:dG mismatch in the correct conformation. Truncated MutY carrying the Lys-142 mutation is a very inefficient catalyst for either dA:dG or dA:8-oxodG substrates and binds DNA very weakly (D.O.Z., unpublished data).

It is noted that the structure of the MutY p25 for which structural information is currently available may be significantly different than that of the full length MutY protein, and the structural interpretations of the biochemical observations may have to be modified accordingly. The most relevant structural arguments relating to the model discussed above would come from a detailed analysis of complexes between the full-length MutY enzyme and duplex DNA.

Despite its reduced ability to process dA:dG mispairs, MutY K142Q complements the *mutY* mutator phenotype of *E. coli* with the same efficiency as wild-type protein. The rifampicin resistance assay (*33*) measures the rate of spontaneous mutations in the gene for bacterial RNA polymerase. Our results indicate that dA:8-oxodG mispairs are much more prominent sources of mutations, at least for this particular locus, than dA:dG mispairs. Several (not mutually exclusive) explanations of this effect are possible. First, the number of dA:8-oxodG mispairs may be higher. While dA:dG mispairs arise from recombination and from misincorporation of purines from the nucleotide triphosphate pool, dA:8-oxodG mispairs result from incorporation of 8-oxodGTP from the triphosphate pool and by misincorporation of dA opposite template 8-oxodG. DNA polymerases discriminate strongly against misincorporation of undamaged triphosphates, but allow relatively efficient incorporation of 8-oxo-dGTP opposite dA and dATP opposite 8-oxodG (*3*, *5*). Second, once the mispair is formed, dA:dG becomes a substrate not only for MutY, but also for the *dam*-dependent mismatch repair system, while in *E. coli* dA:8-oxodG does not (*16*, *55*). Therefore, excision of adenine from dA:8-oxodG mispairs seems to be a primary function for MutY in vivo while dA:dG-repairing activity probably is dispensable. This conclusion is supported by the results of mutation frequency analysis and rescue experiments in *mutY E. coli* (*11*).

ACKNOWLEDGMENT

We thank Cecilia Torres for synthesis of oligonucleotides used in this study, Erich Bremer for assistance with molecular structure visualization, and Susan Rigby for help in preparing this manuscript. We are grateful to Dr. Joel Sussman for his advice and continuing encouragement during this project.

REFERENCES

1. Kasai, H., and Nishimura, S. (1984) *Nucleic Acids Res. 12*, 2137−2145.
2. Marnett, L. J. (2000) *Carcinogenesis 21*, 361−370.
3. Shibutani, S., Takeshita, M., and Grollman, A. P. (1991) *Nature 349*, 431−434.
4. Cheng, K. C., Cahill, D. S., Kasai, H., Nishimura, S., and Loeb, L. A. (1992) *J. Biol. Chem. 267*, 166−172.
5. Pavlov, Y. I., Minnick, D. T., Izuta, S., and Kunkel, T. A. (1994) *Biochemistry 33*, 4695−4701.
6. Michaels, M. L., and Miller, J. H. (1992) *J. Bacteriol. 174*, 6321−6325.
7. Grollman, A. P., and Moriya, M. (1993) *Trends Genet. 9*, 246−249.
8. Maki, H., and Sekiguchi, M. (1992) *Nature 355*, 273−275.
9. Tchou, J., Kasai, H., Shibutani, S., Chung, M.-H., Laval, J., Grollman, A. P., and Nishimura, S. (1991) *Proc. Natl. Acad. Sci. U.S.A. 88*, 4690−4694.
10. Michaels, M. L., Tchou, J., Grollman, A. P., and Miller, J. H. (1992) *Biochemistry 31*, 10964−10968.
11. Michaels, M. L., Cruz, C., Grollman, A. P., and Miller, J. H. (1992) *Proc. Natl. Acad. Sci. U.S.A. 89*, 7022−7025.
12. Lu, A.-L., and Chang, D.-Y. (1988) *Cell 54*, 805−812.
13. Au, K. G., Clark, S., Miller, J. H., and Modrich, P. (1989) *Proc. Natl. Acad. Sci. U.S.A. 86*, 8877−8881.
14. Lu, A.-L., Tsai-Wu, J.-J., and Cillo, J. (1995) *J. Biol. Chem. 270*, 23582−23588.
15. Bulychev, N. V., Varaprasad, C. V., Dormán, G., Miller, J. H., Eisenberg, M., Grollman, A. P., and Johnson, F. (1996) *Biochemistry 35*, 13147−13156.
16. Moriya, M., and Grollman, A. P. (1993) *Mol. Gen. Genet. 239*, 72−76.
17. Michaels, M. L., Pham, L., Nghiem, Y., Cruz, C., and Miller, J. H. (1990) *Nucleic Acids Res. 18*, 3841−3845.
18. Guan, Y., Manuel, R. C., Arvai, A. S., Parikh, S. S., Mol, C. D., Miller, J. H., Lloyd, R. S., and Tainer, J. A. (1998) *Nat. Struct. Biol. 5*, 1058−1064.
19. Thayer, M. M., Ahern, H., Xing, D., Cunningham, R. P., and Tainer, J. A. (1995) *EMBO J. 14*, 4108−4120.
20. Sun, B., Latham, K. A., Dodson, M. L., and Lloyd, R. S. (1995) *J. Biol. Chem. 270*, 19501−19508.
21. Lu, A.-L., Yuen, D. S., and Cillo, J. (1996) *J. Biol. Chem. 271*, 24138−24143.
22. Manuel, R. C., and Lloyd, R. S. (1997) *Biochemistry 36*, 11140−11152.
23. Zharkov, D. O., and Grollman, A. P. (1998) *Biochemistry 37*, 12384−12394.
24. Williams, S. D., and David, S. S. (1998) *Nucleic Acids Res. 26*, 5123−5133.
25. David, S. S., and Williams, S. D. (1998) *Chem. Rev. 98*, 1221−1261.
26. Williams, S. D., and David, S. S. (1999) *Biochemistry 38*, 15417−15424.
27. Bodepudi, V., Shibutani, S., and Johnson, F. (1992) *Chem. Res. Toxicol. 5*, 608−617.
28. Johnson, F., Dormán, G., Rieger, R. A., Marumoto, R., Iden, C. R., and Bonala, R. (1998) *Chem. Res. Toxicol. 11*, 193−202.

29. Takeshita, M., Chang, C.-N., Johnson, F., Will, S., and Grollman, A. P. (1987) *J. Biol. Chem. 262*, 10171−10179.
30. Gerchman, S. E., Graziano, V., and Ramakrishnan, V. (1994) *Protein Expr. Purif. 5*, 242−251.
31. Doublié, S. (1997) *Methods Enzymol. 276*, 523−530.
32. Nghiem, Y., Cabrera, M., Cupples, C. G., and Miller, J. H. (1988) *Proc. Natl. Acad. Sci. U.S.A. 85*, 2709−2713.
33. Miller, J. H. (1992) *A Short Course in Bacterial Genetics: a Laboratory Manual and Handbook for Escherichia coli and Related Bacteria*, Cold Spring Harbor Laboratory Press, Cold Spring Harbor, NY.
34. Porello, S. L., Leyes, A. E., and David, S. S. (1998) *Biochemistry 37*, 14756−14764.
35. Otwinowski, Z., and Minor, W. (1997) *Methods Enzymol. 276*, 307−326.
36. Brünger, A. T., Adams, P. D., Clore, G. M., DeLano, W. L., Gros, P., Grosse-Kunstleve, R. W., Jiang, J. S., Kuszewski, J., Nilges, M., Pannu, N. S., Read, R. J., Rice, L. M., Simonson, T., and Warren, G. L. (1998) *Acta Crystallogr. D 54*, 905−921.
37. Brünger, A. T. (1992) *Nature 355*, 472−475.
38. Jones, T. A., Zou, J.-Y., Cowan, S. W., and Kjeldgaard, M. (1998) *Acta Crystallogr. A A47*, 110−119.
39. Kraulis, P. J. (1991) *J. Appl. Crystallogr. 24*, 946−950.
40. Wright, P. M., Yu, J., Cillo, J., and Lu, A.-L. (1999) *J. Biol. Chem. 274*, 29011−29018.
41. *pET System Manual* (1999), Novagen, Inc.
42. Tsai-Wu, J.-J., Liu, H.-F., and Lu, A.-L. (1992) *Proc. Natl. Acad. Sci. U.S.A. 89*, 8779−8783.
43. Porello, S. L., Williams, S. D., Kuhn, H., Michaels, M. L., and David, S. S. (1996) *J. Am. Chem. Soc. 118*, 10684−10692.
44. Noll, D. M., Gogos, A., Granek, J. A., and Clarke, N. D. (1999) *Biochemistry 38*, 6374−6379.
45. Chepanoske, C. L., Porello, S. L., Fujiwara, T., Sugiyama, H., and David, S. S. (1999) *Nucleic Acids Res. 27*, 3197−3204.
46. Kouchakdjian, M., Bodepudi, V., Shibutani, S., Eisenberg, M., Johnson, F., Grollman, A. P., and Patel, D. J. (1991) *Biochemistry 30*, 1403−1412.
47. McAuley-Hecht, K. E., Leonard, G. A., Gibson, N. J., Thomson, J. B., Watson, W. P., Hunter, W. N., and Brown, T. (1994) *Biochemistry 33*, 10266−10270.
48. Privé, G. G., Heinemann, U., Chandrasegaran, S., Kan, L.-S., Kopka, M. L., and Dickerson, R. E. (1987) *Science 238*, 498−504.
49. Carbonnaux, C., van der Marel, G. A., van Boom, J. H., Guschlbauer, W., and Fazakerley, G. V. (1991) *Biochemistry 30*, 5449−5458.
50. Manuel, R. C., Czerwinski, E. W., and Lloyd, R. S. (1996) *J. Biol. Chem. 271*, 16218−16226.
51. Gogos, A., Cillo, J., Clarke, N. D., and Lu, A.-L. (1996) *Biochemistry 35*, 16665−16671.
52. Volk, D. E., House, P. G., Thiviyanathan, V., Luxon, B. A., Zhang, S., Lloyd, R. S., and Gorenstein, D. G. (2000) *Biochemistry 39*, 7331−7336.
53. Uesugi, S., and Ikehara, M. (1977) *J. Am. Chem. Soc. 99*, 3250−3253.
54. Hickerson, R. P., Chepanoske, C. L., Williams, S. D., David, S. S., and Burrows, C. J. (1999) *J. Am. Chem. Soc. 121*, 9901−9902.
55. Rasmussen, L. J., and Samson, L. (1996) *Carcinogenesis 17*, 2085−2088.

BI001538K